IOP Publishing — Journal of Physics A: Mathematical and Theoretical

J. Phys. A: Math. Theor. **48** (2015) 125202 (15pp) doi:10.1088/1751-8113/48/12/125202

Curvature effects in statics and dynamics of low dimensional magnets

Denis D Sheka[1,3], Volodymyr P Kravchuk[2] and Yuri Gaididei[2]

[1] Taras Shevchenko National University of Kiev, 01601 Kiev, Ukraine
[2] Bogolyubov Institute for Theoretical Physics, 03143 Kiev, Ukraine

E-mail: sheka@univ.net.ua, vkravchuk@bitp.kiev.ua and ybg@bitp.kiev.ua

Received 3 November 2014, revised 27 January 2015
Accepted for publication 2 February 2015
Published 2 March 2015

Abstract

We develop an approach to treat magnetic energy of a ferromagnet for arbitrary curved wires and shells on the assumption that the anisotropy contribution greatly exceeds the dipolar and other weak interactions. We show that the curvature induces two effective magnetic interactions: effective magnetic anisotropy and an effective Dzyaloshinskii-like interaction. We derive an equation of magnetization dynamics and propose a general static solution for the limit case of strong anisotropy. To illustrate our approach, we consider the magnetization structure in a ring wire and a cone surface: ground states in both systems essentially depend on the curvature, excluding strictly tangential solutions for a cone surface even in the case of strong anisotropy. We derive also the spectrum of spin waves in such systems.

Keywords: classical spin models, curvature, nanowire, nanoshell

(Some figures may appear in colour only in the online journal)

1. Introduction

An interplay between the topology of the order parameter field and the geometry of the underlying substrate attracts the attention of many researchers in the modern physics of condensed matter and in field theories. One of the well-known examples of the nonlinear vector field model is a general Ginzburg–Landau vector model with the energy functional [1]

$$E = \int \mathrm{d}\boldsymbol{x}\,[\nabla\boldsymbol{u} : \nabla\boldsymbol{u} + V(\boldsymbol{u})] \tag{1}$$

[3] Author to whom any correspondence should be addressed.

for the vector order parameter $\boldsymbol{u} = \left(u^1, u^2, ..., u^n\right)$ in the multidimensional real space $\boldsymbol{x} \in \mathbb{R}^d$, where double-dot denotes a scalar product in both real and order parameter spaces. If transformations of the order parameter and transformations of the real space are independent, the double-dot scalar product is computed in such a way that the vector components in both spaces do not mix: $\nabla\boldsymbol{u}:\nabla\boldsymbol{u} = G_{ij}\nabla u^i\ \nabla u^j$, with G_{ij} being a metric tensor of the order parameter space. A behaviour of vector fields in a curved space [2, 3] becomes more sophisticated due to the intimate relation between the geometry of the substrate space ($\boldsymbol{x}$-variable) and the geometry of the field ($\boldsymbol{u}$-variable). In most studies the vector field was supposed to be strictly tangential to the curved substrate. For example, this assumption was used when the role of curvature in the interaction between defects was studied in two-dimensional (2D) *XY*-like models, which can describe thin layers of superfluids, superconductors, and liquid crystals deposited on curved surfaces [4].

Nowadays there is a growing interest in low-dimensional magnetic objects such as magnetic nanoshells and nanowires. This interest is supported by great advantages in nanotechnology, including numerous magnetic devices (high-density data storage, logic, sensing devices, etc). The theoretical description of the evolution of magnetization structures in such systems is based on the dynamics of a three-dimensional (3D) vector order parameter, such as magnetization unit vector $\boldsymbol{m}$ in a constrained physical space, e.g., a quasi 2D nanoshell and a quasi one-dimensional (1D) nanowire. The interrelation between the topological properties of magnetic structures and the underlying curvature complicates an analysis; nevertheless, it can be a source of new effects. For example, 2π-skyrmions can appear in Heisenberg isotropic magnets due to a coupling between the magnetic field and the curvature of the surface [5]; in easy-surface Heisenberg magnets, the curvature of the underlying surface leads to a coupling between the localized out-of-surface component of the magnetic vortex with its delocalized in-surface structure [6]. It is well known that the curvature of the system can induce an additional effective energy contribution, a so-called 'geometrical potential': In a seminal paper [7] da Costa developed a quantum mechanical approach to study the tangential motion of a particle rigidly bounded to a surface. Similar 'geometrical potential' appears in 1D curved quantum wires [8]. Effects of effective anisotropy induced by the curvature were also discussed for quasi 1D curved magnetic nanowires of particular geometries [9, 10]. In general, the influence of the 'geometrical potential' is 'proportional to the second degree of curvature of the system' [8]. In spite of numerous results on the behaviour of a vector field in curved systems (see, e.g., review articles [2, 3],) the problem is not fully understood. In particular, the 3D vector field in a majority of studies was assumed to be rigidly bound to the surface in the case of magnetic shells or to the curve in the case of magnetic wires.

Very recently we have developed a fully 3D approach for thin magnetic shells of arbitrary shape [11]. In this paper we extend this approach for both 2D shells and 1D wires. We base our study on the phenomenological Landau–Lifshitz equation

$$\partial_t \boldsymbol{m} = \omega_0\, \boldsymbol{m} \times \frac{\delta E}{\delta \boldsymbol{m}}, \tag{2}$$

which describes classical magnetization dynamics. Here E is the total energy normalized by $4\pi M_s^2$ with M_s, being the saturation magnetization. The characteristic time scale of the system is determined by the frequency $\omega_0 = 4\pi\gamma_0 M_s$, with γ_0 being the gyromagnetic ratio. The damping is neglected. For an arbitrary orthogonal basis $\{\boldsymbol{e}_1, \boldsymbol{e}_2, \boldsymbol{e}_3\}$ one can parameterize the unit magnetization vector as follows

$$\boldsymbol{m} = \sin\theta\cos\phi\,\boldsymbol{e}_1 + \sin\theta\sin\phi\,\boldsymbol{e}_2 + \cos\theta\,\boldsymbol{e}_3, \tag{3}$$

where angular variables θ and ϕ depend on spatial and temporal coordinates. Within the angular representation (3), the equation of motion (2) reads

$$\sin\theta\partial_t\phi = \omega_0\frac{\delta E}{\delta\theta}, \qquad -\sin\theta\partial_t\theta = \omega_0\frac{\delta E}{\delta\phi}. \tag{4}$$

The total energy of the magnet can collect different contributions such as energies of exchange, anisotropy, and dipolar one. In the following we consider a hard magnet where the anisotropy contribution greatly exceeds the dipolar and other weak interactions. Therefore in the current study we restrict ourselves to the consideration of Heisenberg magnets. In this case the total energy functional has the following form:

$$E = \int \mathrm{d}V\Big[\ell^2\mathscr{E}_{\text{ex}} + \lambda(\boldsymbol{m}\cdot\boldsymbol{n})^2\Big]. \tag{5}$$

Here the first term describes the isotropic exchange interaction (see below, equation (9)), with $\ell = \sqrt{A/(4\pi M_s^2)}$ being an exchange length and A being an exchange constant. The second term in (5) is the energy of anisotropy. The unit vector $\boldsymbol{n}$ gives the direction of the anisotropy axis, λ is a dimensionless anisotropy constant, and integration is performed over the sample volume V.

An important point is that the vector $\boldsymbol{n}(\boldsymbol{r})$ is a function of spatial coordinates in accordance with the geometry of the curvilinear sample. For example, if $\boldsymbol{n}$ is normal to a curvilinear shell and $\lambda > 0$, then we have a case of easy-surface anisotropy; if $\boldsymbol{n}$ is tangential to a curvilinear wire and $\lambda < 0$, then we have a case of easy-tangential anisotropy, etc. Actually, this is one way of how the curvature is introduced to the problem.

Anisotropic curvilinear systems (5) with a nontrivial topology are of particular interest, since topologically nontrivial magnetization distributions are inherent here. Examples are magnetic vortices in easy-surface spherical shells [6], and magnetic domains in Möbius rings with easy-normal anisotropy [12, 13].

A natural way to look for magnetization distributions in the curvilinear systems is to proceed to the corresponding curvilinear basis. However, the representation of the exchange contribution $\mathscr{E}_{\text{ex}}$ in an *arbitrary* curvilinear frame of reference is quite a challenge. Previously this problem was solved for a couple of simple geometries, namely, cylindrical [14] and spherical [6]. In the present work we propose a general approach to derive the exchange energy for arbitrary curvilinear 1D and 2D systems (curved wires and curved shells) and an arbitrary magnetization vector field, not necessarily tangential to the surface, as it was recently considered for nematic shells [15, 16]. We show that in curvilinear systems there appear two effective magnetic interactions: (i) curvature-induced effective anisotropy, which is bilinear with respect to the curvature and the torsion and is similar to the 'geometrical potential', (ii) curvature-induced effective Dzyaloshinskii-like interaction, which is linear with respect to the curvature and the torsion.

The paper is organized as follows. We derive the energy of the curved 1D wire in section 2; our approach is illustrated by the calculation of the ground state of a highly anisotropic curved wire. In section 3 we discuss the role of the effective anisotropy and the effective Dzyaloshinskii-like interaction for a 2D curved shell. We consider two applications of our theory: the ground state of the narrow ring wire and the spectrum of spin-waves are calculated in section 4, and the spin-wave spectrum for the cone shell is derived in section 5. In section 6 we present some remarks about possible perspectives. Another representation of the energy of 1D wire is proposed in appendix.

2. Energy and curvature-induced effective fields for a curved wire

We start with a 1D case and consider a thin nanowire whose transverse size is small enough to ensure magnetization uniformity along the crosswise direction. One can describe a wire using the Frenet–Serret parametrization for a 3D curve $\boldsymbol{\gamma}$. We use its natural parametrization by arc length s of general form $\boldsymbol{\gamma} = \boldsymbol{\gamma}(s)$. In Cartesian basis $\hat{\boldsymbol{x}}_i \in \{\hat{\boldsymbol{x}}, \hat{\boldsymbol{y}}, \hat{\boldsymbol{z}}\}$, one can parameterize the curve as $\boldsymbol{\gamma} = \gamma_i \hat{\boldsymbol{x}}_i$. The Einstein summation convention is used here and everywhere below. Let us introduce the local normalized curvilinear basis (Frenet–Serret frame):

$$\boldsymbol{e}_1 = \boldsymbol{\gamma}', \qquad \boldsymbol{e}_2 = \frac{\boldsymbol{e}_1'}{\left|\boldsymbol{e}_1'\right|}, \qquad \boldsymbol{e}_3 = \boldsymbol{e}_1 \times \boldsymbol{e}_2 \tag{6}$$

with $\boldsymbol{e}_1$ being the tangent, $\boldsymbol{e}_2$ being the normal, and $\boldsymbol{e}_3$ being the binormal to the curve $\boldsymbol{\gamma}$. Here and below, the prime denotes the derivative with respect to the arc length s. Note that $|\boldsymbol{\gamma}'(s)| = 1$ in the natural parametrization. The differential properties of the curve are determined by the Frenet–Serret formulae:

$$\boldsymbol{e}_\alpha' = F_{\alpha\beta}\boldsymbol{e}_\beta, \qquad \left\|F_{\alpha\beta}\right\| = \begin{pmatrix} 0 & \kappa & 0 \\ -\kappa & 0 & \tau \\ 0 & -\tau & 0 \end{pmatrix}, \tag{7}$$

where κ is the curvature of the wire and τ is its torsion. Latin indices $i, j = 1, 2, 3$ describe the Cartesian coordinates and the Cartesian components of vector fields, whereas Greek indices $\alpha, \beta = 1, 2, 3$ numerate the curvilinear coordinates and the curvilinear components of vector fields.

After defining the 3D curve, one can parameterize a physical wire with a finite crosswise size. We take $\boldsymbol{\gamma}(s)$ as the central curve of a wire. Then the space domain filled by the wire can be parameterized as

$$\boldsymbol{r}\left(s, \xi_2, \xi_3\right) = \boldsymbol{\gamma}(s) + \xi_2\boldsymbol{e}_2 + \xi_3\boldsymbol{e}_3, \tag{8}$$

where $\boldsymbol{\xi} = (\xi_2, \xi_3)$ are coordinates within the cross section $|\boldsymbol{\xi}| \lesssim h$, with h being the wire thickness. The assumption of the magnetization one-dimensionality can be formalized as $\boldsymbol{m} = \boldsymbol{m}(s)$. This assumption is appropriate for cases when the thickness h does not exceed the characteristic magnetic length. We also suppose that $h \ll 1/\kappa, 1/\tau$.

We base our study on the the energy functional (5). In the Cartesian frame of reference, the exchange energy density has the form

$$\mathscr{E}_{\text{ex}} = \left(\nabla m_i\right)\left(\nabla m_i\right). \tag{9}$$

Now one can express the Cartesian components of the magnetization vector m_i in terms of the curvilinear components m_α as follows

$$m_i = m_\alpha\left(\boldsymbol{e}_\alpha \cdot \hat{\boldsymbol{x}}_i\right). \tag{10}$$

Then we substitute this expression into $\mathscr{E}_{\text{ex}}$ and apply a del operator in its curvilinear form, $\nabla \equiv \boldsymbol{e}_1\partial_s$. Finally the energy density in the Frenet–Serret frame of reference reads

$$\mathscr{E}_{\text{ex}} = (m_\alpha\boldsymbol{e}_\alpha)'(m_\beta\boldsymbol{e}_\beta)' = \mathscr{E}_{\text{ex}}^0 + \mathscr{E}_{\text{ex}}^A + \mathscr{E}_{\text{ex}}^D. \tag{11a}$$

Here the first term describes the common isotropic part of the exchange expression, which has formally the same form as for the straight wire

$$\mathscr{E}_{\text{ex}}^0 = m_\alpha' m_\alpha' = |\boldsymbol{m}'|^2. \tag{11b}$$

The second term $\mathscr{E}_{\text{ex}}^{A}$ describes an effective anisotropy-like interaction,

$$\mathscr{E}_{\text{ex}}^{A} = K_{\alpha\beta} m_\alpha m_\beta, \quad K_{\alpha\beta} = F_{\alpha\gamma} F_{\beta\gamma}, \quad \left|\left| K_{\alpha\beta} \right|\right| = \begin{pmatrix} \kappa^2 & 0 & -\kappa\tau \\ 0 & \kappa^2 + \tau^2 & 0 \\ -\kappa\tau & 0 & \tau^2 \end{pmatrix}. \tag{11c}$$

Components of the tensor $K_{\alpha\beta}$ are bilinear with respect to the curvature κ and the torsion τ; they play the role of effective anisotropy coefficients, induced by the curvature of the wire. In some sense it is similar to the 'geometrical potential' which an electron experiences in a curved quantum wire [8]. Note that an effective 'geometrical' magnetic field was calculated recently in curved magnonic waveguides [9]. As opposed to previous studies, we will show below that the curvature and torsion can cause a new magnetization ground state, which is absent in the straight case.

The last term (11c) is a combination of Lifshitz invariants

$$\mathscr{E}_{\text{ex}}^{D} = F_{\alpha\beta} \left(m_\alpha m_\beta' - m_\alpha' m_\beta \right) \tag{11d}$$

and therefore can be interpreted as an effective Dzyaloshinskii interaction [17, 18]. The tensor of coefficients of this effective Dzyaloshinskii interaction $F_{\alpha\beta}$ is exactly the Frenet transformation matrix (see (7)), which is linear with respect to the curvature κ and the torsion τ. Due to the linear form, this term can cause phenomena that depend on the sign of κ and τ.

Using the angular notations (3), one can rewrite the energy terms as follows:

$$\begin{aligned} \mathscr{E}_{\text{ex}}^{0} &= \theta'^2 + \sin^2\theta\phi'^2, \\ \mathscr{E}_{\text{ex}}^{A} &= (\kappa\sin\theta - \tau\cos\theta\cos\phi)^2 + \tau^2\sin^2\phi \\ \mathscr{E}_{\text{ex}}^{D} &= \phi'\left(2\kappa\sin^2\theta - \tau\sin 2\theta\cos\phi\right) - 2\tau\theta'\sin\phi. \end{aligned} \tag{12}$$

Finally, by summing up all terms in (12), we get

$$\mathscr{E}_{\text{ex}}^{1d} = \left[\theta' - \tau\sin\phi\right]^2 + \left[\sin\theta\left(\phi' + \kappa\right) - \tau\cos\theta\cos\phi\right]^2. \tag{13}$$

Note that the exchange magnetic energy of a curved wire was recently calculated in reference [19]. However, curvature effects were ignored, and the exchange energy was written in the form $\mathscr{E}_{\text{ex}}^{0}$. For some applications, e.g., studying domain wall dynamics, it is useful to rewrite the energy (13), using another angular parametrization, where the polar angle θ is counted from the tangential direction (see appendix).

Let us take into account the anisotropy term in (5). We choose the anisotropy axis along the central line of the wire, $\boldsymbol{n} = \boldsymbol{e}_1$. The total energy density, according to (5) has the form:

$$\mathscr{E}^{1d} = \ell^2 \mathscr{E}_{\text{ex}}^{1d} + \lambda\sin^2\theta\cos^2\phi. \tag{14}$$

This developed approach enables us to obtain a general static solution for the high-anisotropy case. We consider a physically interesting case of easy-tangential anisotropy $\lambda < 0$, which favours the magnetization distribution tangential to the wire. In the strong anisotropy limit, the magnetization is quasitangential; therefore $\theta = \pi/2 + \vartheta$, and $|\vartheta|, |\phi| \ll 1$. Then the total energy density can be rewritten as follows

$$\mathscr{E}^{1d} \approx \mathscr{E}_{\text{ex}}^{0} + \underbrace{2\ell^2\left(\tau\kappa\vartheta - \kappa'\phi\right)}_{\mathscr{E}^F} + |\lambda|\left(\vartheta^2 + \phi^2\right) + \text{const}, \tag{15}$$

where the first summand is the energy density of a strictly tangential distribution, and the second summand can be written as $\mathscr{E}^F = -(\boldsymbol{F} \cdot \boldsymbol{m})$. Therefore one can consider it as an interaction with an effective curvature-induced magnetic field

$$\boldsymbol{F} = 2\ell^2 \left(\kappa' \boldsymbol{e}_2 + \tau\kappa \boldsymbol{e}_3 \right), \tag{16}$$

and the last summand in (15) represents the anisotropy contribution. Minimization of the energy functional (15) with respect to ϑ and ϕ results in

$$\theta = \frac{\pi}{2} - \frac{\ell^2}{|\lambda|}\kappa\tau + \mathcal{O}\left(\frac{1}{|\lambda|^2} \right), \qquad \phi = \frac{\ell^2}{|\lambda|}\kappa' + \mathcal{O}\left(\frac{1}{|\lambda|^2} \right). \tag{17}$$

According to (17), the strictly tangential solution is realized only for a specific case $\tau = 0$ and $\kappa' = 0$. Note that in the main part of recent studies of magnetization states in curved nanowires, only the tangential magnetization distributions were considered [9, 10]. The solution for the ground state of 1D magnets (17) is in agreement with recent results for 2D surfaces [11].

3. Energy and the curvature-induced effective fields for a curved shell

In this section we consider the curvature-induced effects in a magnetic nanoshell using a thin-shell limit. We describe a shell considering a surface $\vec{\varsigma}(\xi_1, \xi_2)$, with ξ_1 and ξ_2 being local curvilinear coordinates on the surface. In the Cartesian basis $\hat{\boldsymbol{x}}_i \in \{\hat{\boldsymbol{x}}, \hat{\boldsymbol{y}}, \hat{\boldsymbol{z}}\}$, one can parameterize the surface as $\vec{\varsigma} = \vec{\varsigma}_i \hat{\boldsymbol{x}}_i$. We define the local curvilinear basis as follows:

$$\boldsymbol{e}_1 = \frac{\boldsymbol{g}_1}{|\boldsymbol{g}_1|}, \quad \boldsymbol{e}_2 = \frac{\boldsymbol{g}_2}{|\boldsymbol{g}_2|}, \quad \boldsymbol{e}_3 = \boldsymbol{e}_1 \times \boldsymbol{e}_2, \quad \boldsymbol{g}_\mu = \partial_\mu \boldsymbol{\varsigma}, \tag{18}$$

where $\partial_\mu = \partial / \partial \xi_\mu$, with $\mu = 1, 2$. Similar to notations of the previous section, Greek indices $\alpha, \beta, \gamma = 1, 2, 3$ numerate curvilinear coordinates and curvilinear components of vector fields. To indicate only in-surface curvilinear coordinates, we use Greek notations $\eta, \mu, \nu = 1, 2$. We suppose that the surface curvilinear frame $\{\boldsymbol{e}_1, \boldsymbol{e}_2\}$ is an orthogonal one; hence the surface metric tensor $g_{\mu\nu} = \boldsymbol{g}_\mu \cdot \boldsymbol{g}_\nu$ has a diagonal form, $\| g_{\mu\nu} \| = \mathrm{diag}\left(g_{11}, g_{22} \right)$. The local curvilinearity of the basis $\boldsymbol{e}_\mu$ is determined by the second fundamental form $b_{\mu\nu} = \boldsymbol{e}_3 \cdot \partial_\nu \boldsymbol{g}_\mu$. The Gauss curvature is $\mathcal{K} = \det(H_{\alpha\beta})$, and the mean curvature is $\mathcal{H} = \mathrm{Tr}\,(H_{\alpha\beta})/2$, with the Hessian matrix given by $||H_{\mu\nu}|| = ||b_{\mu\nu} / \sqrt{g_{\mu\mu} g_{\nu\nu}}\,||$.

The differential properties of the curvilinear basis are determined by the Gauss–Codazzi equation

$$\partial_\mu \boldsymbol{g}_\nu = b_{\mu\nu} \boldsymbol{e}_3 + \left\{ \begin{matrix} \eta \\ \mu\nu \end{matrix} \right\} \boldsymbol{g}_\eta \tag{19}$$

with $\left\{ \begin{matrix} \eta \\ \mu\nu \end{matrix} \right\}$ being the Christoffel symbol.

Let us parameterize the ferromagnetic shell using the thin-shell limit. Considering the surface $\vec{\varsigma}(\xi_1, \xi_2)$ as the central surface of a shell, we define a finite thickness shell as the following space domain

$$\boldsymbol{r}\left(\xi_1, \xi_2, \xi_3 \right) = \boldsymbol{\varsigma}\left(\xi_1, \xi_2 \right) + \xi_3 \boldsymbol{e}_3, \tag{20}$$

where $\xi_3 \in [-h/2, h/2]$ are the cross-section coordinates, with h being the shell thickness. Similarly to the previous section, we use the assumption that the thickness h is infinitesimally small and suppose that the magnetization does not depend on ξ_3; hence $\boldsymbol{m} = \boldsymbol{m}(\xi_1, \xi_2)$.

In order to calculate the exchange energy of the shell, we start with the definition (9) and substitute the Cartesian components of the magnetization vector m_i in terms of the curvilinear components m_α, as follows $m_i = m_\alpha\left(\boldsymbol{e}_\alpha \cdot \hat{\boldsymbol{x}}_i\right)$. By applying a del operator in its curvilinear form $\nabla \equiv \boldsymbol{e}_\alpha \nabla_\alpha \equiv \boldsymbol{e}_\alpha (g_{\alpha\alpha})^{-1/2}\partial_\alpha$, we get the exchange energy in the form, similar to (11):

$$\mathscr{E}_{\text{ex}} = \nabla_\alpha \boldsymbol{m} \cdot \nabla_\alpha \boldsymbol{m} = \mathscr{E}_{\text{ex}}^0 + \mathscr{E}_{\text{ex}}^A + \mathscr{E}_{\text{ex}}^D. \tag{21a}$$

The first term is the isotropic part of the exchange expression

$$\mathscr{E}_{\text{ex}}^0 = \nabla m_\alpha \cdot \nabla m_\alpha, \tag{21b}$$

which has formally the same form as for the plane surface.

Similarly to the 1D case, the curvature manifests itself in the effective anisotropy-like term $\mathscr{E}_{\text{ex}}^A$ and the effective Dzyaloshinskii interaction term $\mathscr{E}_{\text{ex}}^D$ as follows:

$$\begin{aligned} \mathscr{E}_{\text{ex}}^A &= K_{\alpha\beta} m_\alpha m_\beta, \qquad K_{\alpha\beta} = \nabla_\gamma \boldsymbol{e}_\alpha \cdot \nabla_\gamma \boldsymbol{e}_\beta, \\ \mathscr{E}_{\text{ex}}^D &= 2D_{\alpha\beta\gamma} m_\beta \nabla_\gamma m_\alpha, \qquad D_{\alpha\beta\gamma} = \boldsymbol{e}_\alpha \cdot \nabla_\gamma \boldsymbol{e}_\beta. \end{aligned} \tag{21c}$$

By using the Gauss–Codazzi equation (19), one can show that the components of the tensor $K_{\alpha\beta}$ have a bilinear form with respect to the components of the second fundamental form $b_{\mu\nu}$; it emulates a 'geometrical potential' closely related to the potential that arises in the quantum mechanical problem of the particle rigidly bounded to a surface [7]. The effective Dzyaloshinskii interaction coefficients $D_{\alpha\beta\gamma}$ are linear with respect to the $b_{\mu\nu}$ components. This effective interaction is a source of possible magnetochiral effects, such as the vortex polarity–chirality coupling [6] and the interrelation between chiralities of the sample and its magnetization subsystem for Möbius rings [13]. The effects of curvature-induced magnetochirality were reviewed recently in reference [20].

Let us use the angular parametrization (3), with $\theta = \theta(\xi_1, \xi_2)$ being the colatitude and $\phi = \phi(\xi_1, \xi_2)$ being the azimuthal angle in the local frame of reference. In terms of θ and ϕ, the exchange energy density $\mathscr{E}_{\text{ex}}$ reads

$$\mathscr{E}_{\text{ex}}^{2d} = [\nabla\theta - \boldsymbol{\Gamma}(\phi)]^2 + \left[\sin\theta(\nabla\phi - \boldsymbol{\Omega}) - \cos\theta\frac{\partial\boldsymbol{\Gamma}(\phi)}{\partial\phi}\right]^2. \tag{22}$$

Here the vector $\boldsymbol{\Omega}$ is a modified spin connection, $\boldsymbol{\Omega} = \boldsymbol{e}_\mu(\boldsymbol{e}_1 \cdot \nabla_\mu \boldsymbol{e}_2)$, and vector $\boldsymbol{\Gamma}$ is determined as follows

$$\boldsymbol{\Gamma}(\phi) = \| H_{\alpha\beta} \| \, \boldsymbol{\varepsilon}(\phi) = \mathcal{H}\, \boldsymbol{\varepsilon}(\phi) + \sqrt{\mathcal{H}^2 - \mathcal{K}}\, \boldsymbol{\varepsilon}(\upsilon - \phi), \tag{23}$$

where $\boldsymbol{\varepsilon}(\phi) = (\cos\phi, \sin\phi)$ and $\tan\upsilon = 2H_{12}/(H_{11} - H_{22})$. Very recently we derived the exchange energy for the curved shell in the form (22) in reference [11].

It is instructive to establish a link between the 2D energy (22) and the 1D expression (13). For this purpose we define the surface $\boldsymbol{\sigma}(\xi_1, \xi_2)$ as a local extension of the curve $\boldsymbol{\gamma}(s)$ in the following way

$$\boldsymbol{\varsigma}\left(\xi_1 \equiv s, \xi_2\right) = \boldsymbol{\gamma}(s) + \xi_2 \boldsymbol{e}_2(s). \tag{24}$$

By using the Frenet–Serret formulae (6) and (7), one can easily find the corresponding metric tensor and the Hessian matrix. For points of the curve $\boldsymbol{\gamma}$ one has

$$\lim_{\xi_2 \to 0} \left\| g_{\mu\nu} \right\| = \text{diag}(1, 1), \qquad \lim_{\xi_2 \to 0} \left\| H_{\mu\nu} \right\| = \text{adiag}(\tau, \tau). \tag{25}$$

According to (23) one can find that $\boldsymbol{\Gamma}(\boldsymbol{\gamma}) = \boldsymbol{e}_1 \tau \sin\phi$ and the spin connection $\boldsymbol{\Omega}(\boldsymbol{\gamma}) = -\kappa \boldsymbol{e}_1$. Assuming now that the magnetization on the surface (24) depends on s only, one obtains $\nabla\theta = \theta'(s)\boldsymbol{e}_1$ and $\nabla\phi = \phi'(s)\boldsymbol{e}_1$, and finally the 2D energy (22) takes the form (13).

Let us take into account the anisotropy term, starting from the energy functional (5) and choosing the anisotropy axis $\boldsymbol{n} = \boldsymbol{e}_3$, i.e., along the normal to the surface. Then the total energy density of the shell is

$$\mathscr{E}^{2d} = \ell^2 \mathscr{E}^{2d}_{\text{ex}} + \lambda \cos^2\theta. \tag{26}$$

Similarly to the case of 1D nanowire, the general static solutions for the highly anisotropic 2D shell can be obtained. As previously, this solution can be treated as a result of acting of an effective curvature-induced magnetic field. Since this approach for the 2D case was already discussed in reference [11], we limit ourselves with an example for a positive anisotropy constant, namely $\lambda \gg 1$. This corresponds to strong easy-surface anisotropy. In this case the magnetization has a quasitangential distribution: $\theta = \pi/2 + \vartheta$, with $|\vartheta| \ll 1$. The total energy density reads [11]

$$\begin{aligned} &\mathscr{E}^{2d} \approx \mathscr{E}^{\text{t}} + F\vartheta + \lambda\vartheta^2, \\ &\mathscr{E}^{\text{t}} = \ell^2\left[\boldsymbol{\Gamma}^2 + (\nabla\phi - \boldsymbol{\Omega})^2\right], \qquad F = 2\ell^2\left[\nabla\cdot\boldsymbol{\Gamma} + (\nabla\phi - \boldsymbol{\Omega})\frac{\partial\boldsymbol{\Gamma}}{\partial\phi}\right], \end{aligned} \tag{27}$$

where $\mathscr{E}^{\text{t}}$ is the energy density of the strictly tangential distribution and $F(\phi)$ can be treated as the amplitude of an effective curvature-induced magnetic field oriented along vector $\boldsymbol{\varepsilon}$. Minimization of (27) with respect to ϑ and ϕ results in

$$\theta = \frac{\pi}{2} - \frac{1}{2\lambda}F(\phi) + \mathcal{O}\left(\frac{1}{|\lambda|^2}\right), \tag{28}$$

where the equilibrium function ϕ is obtained as a solution of the equation $\delta\mathscr{E}^{\text{t}}/\delta\phi = 0$. According to (28) the strictly tangential solution is realized only for a specific case $F(\phi) \equiv 0$. Consideration of the case of strong easy-normal anisotropy ($\lambda \ll -1$) can be found in reference [11].

It is worth noticing here that the appearance of an effective Dzyaloshinskii-like interaction (or, in other words, Lifshitz invariants) in curved magnetic systems is inherently coupled with the fact that, in contrast to the order parameter $\boldsymbol{u}$ in the Ginzburg–Landau functional given by equation (1), the magnetization $\boldsymbol{m}$ is a vector which is transformed by transformations of the real space. Formally it is expressed in equation (10), which shows that the coupling between the Cartesian and curvilinear components of the magnetization vector is space dependent, and therefore the action of the del operator on the corresponding coefficients cannot be ignored.

4. 1D example: ground state and magnon spectrum for ring nanowire

As an example of our approach for curved magnets, we consider the magnetization distribution in the simplest curvilinear system with constant curvature and no torsion, i.e., a ring-shaped wire (circumference). Using the arc length coordinate s, we put $\boldsymbol{\gamma}(s) = \left\{\kappa^{-1}\cos(\kappa s), \kappa^{-1}\sin(\kappa s), 0\right\}$. Let us consider the case with easy tangential anisotropy $\lambda < 0$. The total energy (5) of the wire with the area cross-section $\mathcal{S}$ has the form $E = 2\pi\mathcal{S}|\lambda|\kappa^{-1}\mathcal{E}$, where

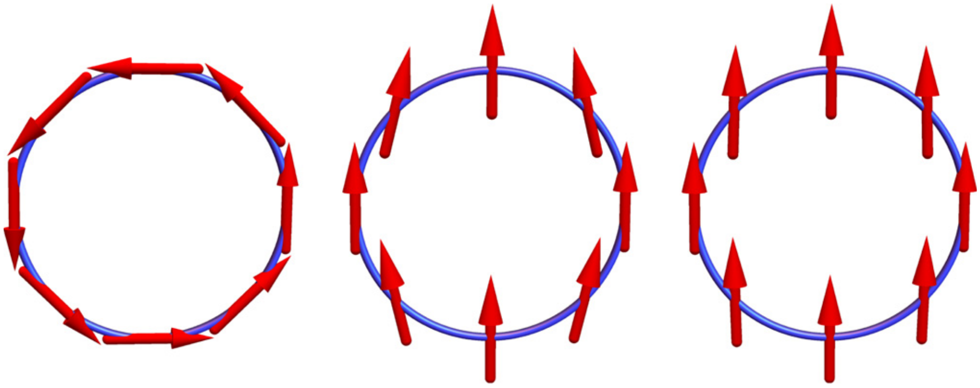

(a) $\varkappa < \varkappa_c$ (b) $\varkappa = 0.7$ (c) $\varkappa = 2$

Figure 1. Magnetization distribution of the ground state in a ring wire with different reduced curvatures $\varkappa$: (a) vortex state, (b) and (c) onion states (32).

$$\mathcal{E} = \frac{1}{2\pi}\int_0^{2\pi}\left\{\varkappa^2\left[\left(\partial_\chi\theta\right)^2 + \sin^2\theta\left(1 - \partial_\chi\Phi\right)^2\right] - \sin^2\theta\sin^2\Phi\right\}\mathrm{d}\chi. \quad (29)$$

Here we used the modified magnetization azimuthal angle $\Phi = \pi/2 - \phi$, the angular variable $\chi \equiv \kappa s$, the reduced curvature $\varkappa \equiv \kappa w$, and the 'magnetic' length $w = \ell/\sqrt{|\lambda|}$. The minimization of the energy (29) results in $\theta = \pi/2$ and the azimuthal angle Φ, which satisfies the pendulum equation

$$\varkappa^2\partial_{\chi\chi}\Phi + \sin\Phi\cos\Phi = 0. \quad (30)$$

The homogeneous (in the curvilinear reference frame) solution corresponds to the planar vortex state:

$$\Phi^{\text{vor}} = \mathcal{C}\frac{\pi}{2}, \qquad \theta^{\text{vor}} = \frac{\pi}{2}, \quad (31)$$

which is well known for the magnetic nanorings [21, 22]; therefore, we name it a *vortex* solution, and the parameter $\mathcal{C} = \pm 1$ is called the vortex chirality (clockwise or counterclockwise). The energy of the vortex state $\mathcal{E}^{\text{vor}} = -1 + \varkappa^2$.

An inhomogeneous solution of the pendulum equation (30) reads

$$\Phi^{\text{on}}(\chi) = \text{am}(x, k), \qquad x = \frac{2\chi}{\pi}\mathrm{K}(k), \qquad \theta^{\text{on}} = \frac{\pi}{2}, \quad (32a)$$

where $\text{am}(x, k)$ is Jacobi's amplitude [23] and the modulus k is determined by the condition

$$2\varkappa k\mathrm{K}(k) = \pi, \quad (32b)$$

with $\mathrm{K}(k)$ being the complete elliptic integral of the first kind [23]. The corresponding magnetization solution is analogous to a well-known onion sate [21, 22] typical for the ring geometry; hence we refer to (32) as the *onion* state. The energy of the onion state reads

$$\mathcal{E}^{\text{on}} = \frac{4\varkappa}{\pi k}\mathrm{E}(k) - \varkappa^2 - \frac{1}{k^2}, \quad (33)$$

where $\mathrm{E}(k)$ is the complete elliptic integral of the second kind [23]. The equality of energies $\mathcal{E}^{\text{vor}} = \mathcal{E}^{\text{on}}$ determines the critical curvature $\varkappa_c \approx 0.657$, which separates the vortex state

($\varkappa < \varkappa_c$) and the onion one ($\varkappa > \varkappa_c$). The typical magnetization distribution is shown in figure 1.

To analyse the magnons in the system, we linearize the Landau–Lifshitz equations (4) on the background of $\theta_0 = \pi/2$ and $\Phi_0(\chi)$, which corresponds to the vortex state ($\Phi_0 = \Phi^{\text{vor}}$) or the onion one ($\Phi_0 = \Phi^{\text{on}}$), depending on the curvature $\varkappa$. For the small deviations $\vartheta = \theta - \theta_0$ and $\varphi = \Phi - \Phi_0(\chi)$, we get the set of linear equations:

$$\left[-\varkappa^2\partial_{\chi\chi} + V_1(\chi)\right]\vartheta = -\partial_\tau\varphi, \quad \left[-\varkappa^2\partial_{\chi\chi} + V_2(\chi)\right]\varphi = \partial_\tau\vartheta, \tag{34a}$$

where ∂_τ is the derivative with respect to dimensionless time $\tau = \Omega_0 t$, with $\Omega_0 = 2\omega_0|\lambda|$. Here the 'potentials' $V_1(\chi)$ and $V_2(\chi)$ are as follows:

$$V_1(\chi) = \sin^2\Phi_0 - \varkappa^2\left[1 - \partial_\chi\Phi_0(\chi)\right]^2, \qquad V_2(\chi) = -\cos 2\Phi_0(\chi). \tag{34b}$$

We apply the partial wave expansion

$$\vartheta(\chi, \tau) = \sum_{m=0}^{\infty}\vartheta_m \cos\left(m\chi - \Omega\tau + \delta_m\right), \quad \varphi(\chi, \tau) = \sum_{m=0}^{\infty}\varphi_m \sin\left(m\chi - \Omega\tau + \delta_m\right) \tag{35}$$

with m being the azimuthal quantum numbers, δ_m being arbitrary phases, and $\Omega = \omega/\Omega_0$ being dimensionless frequencies. Let us mention that equation (34) for the partial waves ϑ_m and φ_m are invariant under the conjugation $\Omega \to -\Omega$, $m \to -m$, $\delta_m \to -\delta_m$, $\vartheta_m \to \vartheta_m$, and $\varphi_m \to -\varphi_m$. In classical theory we can choose any sign of frequency; nevertheless, to make a contact with a quantum mechanics with a positive frequency and energy $\mathscr{E}_k = \hbar\omega_k$, we discuss the case $\Omega > 0$ only.

First we consider the magnons on the background of the vortex state (31). In this case $V_1 = 1 - \varkappa^2$ and $V_2 = 1$. By substituting the expansion (35), into equation (34) one can calculate the following spectrum of magnon eigenstates:

$$\Omega_m^{\text{vor}}(\varkappa) = \sqrt{\left(1 + \varkappa^2 m^2\right)\left(1 + \varkappa^2 m^2 - \varkappa^2\right)}. \tag{36}$$

The lower eigenfrequencies are plotted in the figure 2.

In the limit case of a quasi-straight wire ($\varkappa \to 0$), the magnon frequencies read

$$\Omega_m^{\text{vor}}(\varkappa) = 1 - \frac{\varkappa^2}{2} + \varkappa^2 m^2 + O\left(\varkappa^4\right).$$

Thus the curvature decreases the gap as compared to the case of the straight wire ($\varkappa = 0$) with dispersion $\Omega_s(\mathfrak{K}) = 1 + \mathfrak{K}^2$, where $\mathfrak{K} = \varkappa m$ is the corresponding normalized wave vector.

Let us consider now the magnons on the background of the onion state (32). By substituting $\Phi_0 = \Phi^{\text{on}}$ into (34*b*) one can present the potentials $V_1(\chi)$ and $V_2(\chi)$ as the following Fourier expansions [23]

$$\begin{aligned}
&V_1 = A_0 + \sum_{n=1}^{\infty}A_n\cos(2n\chi), \qquad V_2 = B_0 + \sum_{n=1}^{\infty}B_n\cos(2n\chi),\\
&A_0 = \frac{1}{k^2} - \frac{4}{\pi}\frac{\varkappa}{k}\mathrm{E}(k) + \varkappa^2, \quad A_n = 8\varkappa^2 q^n\left[\frac{1}{1 + q^{2n}} - \frac{2n}{1 - q^{2n}}\right],\\
&B_0 = \frac{2}{k^2} - \frac{4}{\pi}\frac{\varkappa}{k}\mathrm{E}(k) - 1, \quad B_n = -16\varkappa^2\frac{nq^n}{1 - q^{2n}}
\end{aligned} \tag{37}$$

where Jacobi's nome q is given in terms of the modulus k by $q = \exp\left(-\pi\mathrm{K}(\sqrt{1 - k^2})/\mathrm{K}(k)\right)$ [23]. At critical point $\varkappa_c$ the nome $q(\varkappa_c) \approx 0.135$, and its

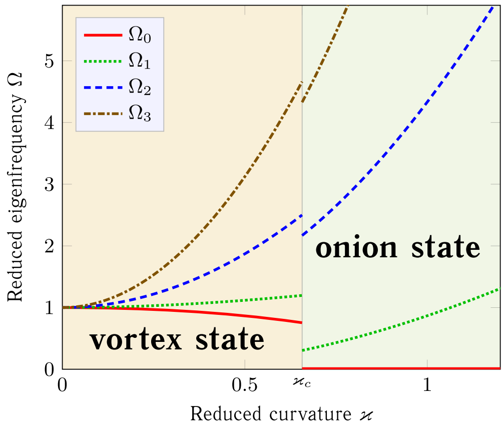

Figure 2. The lowest eigenfrequencies of linear excitations in a ring nanowire depending on the curvature $\varkappa$.

value rapidly tends to zero with $\varkappa$. Thus we can restrict ourselves with few lower Fourier harmonics.

Now by substituting (35) and (37) into (34*a*) and multiplying the Fourier series, we get the following set of equations

$$\begin{aligned} &\left(\varkappa^2 m^2 + A_0\right)\vartheta_m + \frac{1}{2}\sum_{n=1}^{\infty} A_n\left(\vartheta_{m+2n} + \vartheta_{m-2n}\right) = \Omega\varphi_m,\\ &\left(\varkappa^2 m^2 + B_0\right)\varphi_m + \frac{1}{2}\sum_{n=1}^{\infty} B_n\left(\varphi_{m+2n} + \varphi_{m-2n}\right) = \Omega\vartheta_m, \end{aligned} \tag{38}$$

where the conventional rule $f_{-|n|} = f_{|n|}$ is used for the amplitudes ϑ_n and φ_n.

We do not possess the exact solution of the infinite set of equation (38). As a first approach, by neglecting the modes coupling one obtains

$$\Omega_m^{(u)} = \sqrt{\left(\varkappa^2 m^2 + A_0\right)\left(\varkappa^2 m^2 + B_0\right)}. \tag{39}$$

The coupling results in the mixing of different partial waves. However, the influence of coupling decreases with n due to the rapid decay of A_n and B_n; hence (39) provides a good enough estimation of frequencies for not very small azimuthal quantum number m.

An exception is $\Omega = 0$: in this case the zero (Goldstone) mode is realized due to the arbitrary direction of the onion axis. This eigenstate has the following form

$$\varphi^{\mathrm{G}}(\chi) = \partial_\chi \Phi^{\mathrm{on}}(\chi) \propto \mathrm{dn}\,(x, k), \qquad \vartheta^{\mathrm{G}}(\chi) = 0, \qquad \Omega^{\mathrm{G}} = 0. \tag{40}$$

Using the Fourier expansion of Jacobi's function $\mathrm{dn}\,(x, k)$, one can easily see that the Goldstone mode $\varphi^{\mathrm{G}}(\chi)$ contains an infinite number of partial waves; hence the coupling between different partial waves for this mode is crucial. One has to stress that as distinct from the vortex case, eigenstates on the background of the onion state do not coincide with partial waves: each eigenstate with eigenfrequency Ω_n corresponds to a set of partial waves with different azimuthal quantum numbers m due to the coupling. The lowest eigenfrequencies, calculated using (38) with account of only the four lowest partial waves Ω_n, are plotted in figure 2.

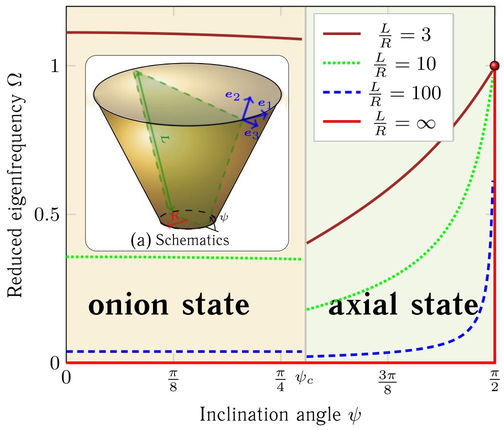

Figure 3. The lowest frequencies of linear excitations over the easy-surface ground states of the cone, depending on the relative generatrix length L/R and inclination angle ψ. Inset (a) shows geometry and notations.

The spectrum of the narrow nanorings is well studied experimentally [24, 25]. It should be noted that for typical experiments ring radii R are about hundreds of nanometres, while the typical magnetic length w is about 10 nanometres; hence the dimensionless curvature $\varkappa \approx w/R \ll 1$. That is why in most experiments the ground state of the ring is the vortex state, and the onion one appears only under the influence of an external magnetic field [21].

One has to stress that we do not discuss here the influence of the dipolar interaction on the magnetization structure, supposing that the thickness is much smaller than the exchange length. Nevertheless it is instructive to compare our results for the critical curvature $\varkappa_c$ with the boundary between different phases in magnetic rings. Our case of circumference–wire corresponds to the very narrow ring. It is well known [26] that depending on the geometrical and magnetic parameters of the nanoring, there exist different magnetic phases in a magnetically soft ring: easy-axis, easy-plane, and planar vortex phases. The lowest bound for the vortex state magnetic ring is given by the triple point $R^{(\text{tr})} \approx \ell\sqrt{3}$ for the infinitesimally narrow ring [26]. For rough estimation of the critical curvature we can simply replace the magnetic length w by the exchange length ℓ; hence $\varkappa \approx \ell/R^{(\text{tr})} = 1/\sqrt{3} \approx 0.577$, which is close to $\varkappa_c \approx 0.657$. One has to note that the monodomain state in [26] was supposed to be the easy-axial one instead of the onion state.

5. 2D example: linear magnetization dynamics for a cone shell

In this section we illustrate our approach for curved shells, considering a cone shell with high easy-surface anisotropy. Recently we found out the ground magnetization states of the side surface of a right circular truncated cone [11]. In the current study we solve the dynamical problem of spin waves on the background of the ground state.

Let us consider the cone surface, where the radius of the truncation face is R and the length of the cone generatrix is L. Varying the generatrix inclination angle $\psi \in [0, \pi/2]$, one can continuously proceed from the planar ring ($\psi = 0$) to the cylinder surface ($\psi = \pi/2$) (for notations see inset (a) in figure 3). The cone surface can be parameterized as follows,

$$x + \mathrm{i}y = \left(R + \xi_2 \cos\psi\right) \exp\left(\mathrm{i}\xi_1\right), \qquad z = \xi_2 \sin\psi, \tag{41}$$

with the curvilinear coordinates $\xi_1 \in S^1$ and $\xi_2 \in [0, L]$. The parametrization (41) generates the following geometrical properties: the metric tensor $\| g_{\alpha\beta} \| = \mathrm{diag}(g;\, 1)$, the modified spin connection $\boldsymbol{\Omega} = \boldsymbol{e}_1 \cos\psi/\sqrt{g}$, and $\boldsymbol{\Gamma} = -\boldsymbol{e}_1 \sin\psi \cos\phi/\sqrt{g}$, where $\sqrt{g} = R + \xi_2 \cos\psi$ [11]. As above, we use here the angular parametrization (3) for the magnetization.

We limit ourselves by the case of the strong easy-surface anisotropy. In accordance to (28), the magnetization polar angle $\theta \approx \pi/2$. Similar to the 1D case, the azimuthal magnetization angle ϕ satisfies the pendulum equation [11] (see (30)),

$$\partial_{\xi_1\xi_1}\phi + \sin^2\psi \sin\phi \cos\phi = 0. \tag{42}$$

The ground state of such a cone is the onion state ϕ^{on} for $\psi < \psi_c \approx 0.8741$ and the axial one ϕ^{ax} for $\psi > \psi_c$ [11]:

$$\phi^{\mathrm{on}}\left(\xi_1\right) = \mathrm{am}(x, k), \qquad x = \frac{2\xi_1}{\pi}\mathrm{K}(k), \qquad \phi^{\mathrm{ax}} = \pm\pi/2, \tag{43}$$

where the modulus k of the Jacobi's amplitude is determined by the condition $2k\mathrm{K}(k) = \pi \sin\psi$ (see (32)). The magnetization dynamics follows the Landau–Lifshitz equation (4). In the case of a high easy-surface anisotropy $\lambda \gg \ell^2/\mathcal{R}^2$, one can derive the dynamical equation for the in-surface magnetization angle ϕ:

$$\frac{\partial_{tt}\phi}{4\lambda\omega_0^2\ell^2} = \nabla \cdot (\nabla\phi - \boldsymbol{\Omega}) - \boldsymbol{\Gamma} \cdot \frac{\partial \boldsymbol{\Gamma}}{\partial\phi}. \tag{44}$$

For the cone surface (41) the dynamic equation (44) takes the form

$$\frac{g}{4\lambda\omega_0^2\ell^2}\partial_{tt}\phi = \partial_{\xi_1\xi_1}\phi + g\partial_{\xi_2\xi_2}\phi + \sqrt{g}\cos\psi\,\partial_{\xi_2}\phi + \frac{1}{2}\sin^2\psi \sin 2\phi. \tag{45}$$

Now after linearizing this equation on the background of the onion state $\phi^{\mathrm{on}}(\xi_1)$, we can present the small deviation $\varphi = \phi - \phi^{\mathrm{on}}$ in the following form:

$$\varphi\left(\xi_1, \xi_2, t\right) = \mathrm{e}^{\mathrm{i}\omega t}\mathrm{P}(\rho)\mathrm{X}(x), \tag{46a}$$

where $\rho = 1 + \frac{\xi_2}{R}\cos\psi$, and x is defined in (43). By separating variables one can find that the angular part $\mathrm{X}(x)$ satisfies the Lamé equation [23]

$$\mathrm{X}'' + \left[\Lambda - 2k^2\,\mathrm{sn}^2(x, k)\right]\mathrm{X} = 0, \tag{46b}$$

where $\mathrm{sn}\,(x, k)$ is a Jacobi elliptic function [23]. The periodic solution of (46*b*), which corresponds to the lowest eigenvalue $\Lambda = k^2$ [23], coincides (up to the constant) with the following Lamé function $\mathrm{X}(x) = \mathcal{C}\mathrm{Ec}_1^0(x, k^2)$. Then the function $\mathrm{P}(\rho)$ appears as the solution $\mathrm{P}(\rho) = \mathcal{C}_1\mathrm{J}_0(\mathrm{q}\rho) + \mathcal{C}_2\mathrm{N}_0(\mathrm{q}\rho)$ of a zero-order Bessel equation, where $\mathrm{q} = \Omega/\cos\psi$, with $\Omega = \omega/\omega_c$ and $\omega_c = 2\omega_0\sqrt{\lambda}\,\ell/R$. Using the boundary conditions

$$\mathrm{P}'(0) = \mathrm{P}'(\rho_0) = 0, \tag{46c}$$

where $\rho_0 = 1 + \frac{L}{R}\cos\psi$, one can determine the eigenvalues from the following equation $\mathrm{J}_1(\mathrm{q})\mathrm{N}_1(\mathrm{q}\rho_0) = \mathrm{J}_1(\mathrm{q}\rho_0)\mathrm{N}_1(\mathrm{q})$, whose numerical solution is plotted in figure 3 for the case $\psi < \psi_c$.

Similar to (40), there is the zero (Goldstone) mode for the magnon oscillations on the onion background. The eigenstate for the zero mode reads:

$$\varphi^{\mathrm{G}}(\xi_1) = X^{\mathrm{G}}(x) = \mathrm{dn}\,(x,\,k), \qquad \Lambda^{\mathrm{G}} = k^2, \qquad \Omega^{\mathrm{G}} = 0. \tag{47}$$

Let us analyse now the spin waves on the background of the axial state $\phi^{\mathrm{ax}} = \pm\pi/2$. Similar to (46) one can find that

$$\phi(\xi_1,\,\xi_2,\,t) \approx \pm\frac{\pi}{2} + \mathrm{e}^{\mathrm{i}\omega t + \mathrm{i}\mu\xi_1}\mathrm{P}(\rho), \qquad \mu \in \mathbb{Z}, \tag{48}$$

where the radial function $\mathrm{P}(\rho) = C_1\mathrm{J}_\nu(\mathrm{q}\rho) + C_2\mathrm{N}_\nu(\mathrm{q}\rho)$, with $\nu = \sqrt{\sin^2\psi + \mu^2}\big/\cos\psi$. The boundary conditions (46*c*) lead to the equation $\mathrm{J}'_\nu(\mathrm{q})\mathrm{N}'_\nu(\mathrm{q}\rho_0) = \mathrm{J}'_\nu(\mathrm{q}\rho_0)\mathrm{N}'_\nu(\mathrm{q})$, which determines the eigenfrequencies. Its numerical solutions for the lowest mode $\mu = 0$ are plotted in figure 3 for the case $\psi > \psi_c$. As well as in the previous case, the lowest frequency becomes arbitrarily small, with the cone size increasing. Nevertheless, it is not so for the cylinder surface, where the lowest frequency is fixed and is equal to ω_c. The case of cylinder ($\psi = \pi/2$) should be considered separately, starting from equation (45), whose linear solution against the axial state has the form $\phi = \pm\pi/2 + C\mathrm{e}^{\mathrm{i}(\omega t + \mu\xi_1 + \mathrm{q}_\parallel\xi_2)}$, with $\mathrm{q}_\parallel$ being the wave vector along the cylinder axis. The corresponding dispersion relation reads $\Omega = \sqrt{1 + \mu^2 + R^2\mathrm{q}_\parallel^2}$. Existence of a gap in the spectrum of the cylindrical magnetic shell was already predicted theoretically [27] and checked by numerical simulations [28].

6. Summary

To conclude, we develop the general approach to describe the magnetization states in arbitrary curved magnetic wires and shells in the vanishing thickness limit. The curvature induces effective magnetic anisotropy and an effective Dzyaloshinskii-like interaction. We obtain an equation of magnetization dynamics and propose a general static solution for the limit case of strong anisotropy. In the latter case the curvature effect is reduced to an influence of effective curvature-induced magnetic fields. We illustrate our approach by two examples: (i) we calculate possible ground states of ring wires and compute the magnon spectrum in this system, and (ii) we study the magnon spectrum in the cone shell. In both cases the curvature is the source of different possible ground states. The curvature contribution to the magnon spectrum of these systems is mostly due to the curvature-induced anisotropy.

Appendix Exchange interaction of the curved wire: another representation

In this appendix we discuss another angular parametrization for the magnetization:

$$\boldsymbol{m} = \cos\Theta\,\boldsymbol{e}_1 + \sin\Theta\cos\Phi\,\boldsymbol{e}_2 + \sin\Theta\sin\Phi\,\boldsymbol{e}_3, \tag{A.1}$$

where $\Theta = \Theta(s)$ and $\Phi = \Phi(s)$ are the angles in the Frenet–Serret frame of reference: the polar angle Θ describes the deviation of magnetization from the tangential curve direction, while the azimuthal angle Φ corresponds to the deviation from the normal. Similar to (12), one can rewrite the energy terms as follows:

$$\begin{aligned}
\mathscr{E}_{\mathrm{ex}}^{0} &= (\nabla\Theta)^2 + \sin^2\Theta(\nabla\Phi)^2,\\
\mathscr{E}_{\mathrm{ex}}^{A} &= (\kappa\cos\Theta\sin\phi - \tau\sin\Theta)^2 \ + \kappa^2\cos^2\Phi\\
\mathscr{E}_{\mathrm{ex}}^{D} &= 2\Phi'\sin\Theta(\tau\sin\Theta - \kappa\cos\Theta\sin\Phi) + 2\kappa\Theta'\cos\Phi.
\end{aligned} \tag{A.2}$$

Finally, the exchange energy takes the form (see (13))

$$\mathscr{E}_{\text{ex}} = \left(\Theta' + \kappa \cos \Phi\right)^2 + \left[\sin \Theta\left(\Phi' + \tau\right) - \kappa \cos \Theta \sin \Phi\right]^2. \tag{A.3}$$

References

[1] Pismen L M 1999 *Vortices in Nonlinear Field* (Oxford: Oxford University Press)
[2] Bowick M J and Giomi L 2009 *Adv. Phys.* **58** 449–563
[3] Turner A M, Vitelli V and Nelson D R 2010 *Rev. Mod. Phys.* **82** 1301–48
[4] Vitelli V and Turner A M 2004 *Phys. Rev. Lett.* **93** 215301
[5] Carvalho-Santos V L and Dandoloff R 2012 *Phys. Lett.* A **376** 3551–4
[6] Kravchuk V P, Sheka D D, Streubel R, Makarov D, Schmidt O G and Gaididei Y 2012 *Phys. Rev.* B **85** 144433
[7] da Costa R C T 1981 *Phys. Rev.* A **23** 1982–7
[8] Magarill L I, Chaplik A V and Entin M V 2005 *Phys.—Usp.* **48** 953–8
[9] Tkachenko V S, Kuchko A N, Dvornik M and Kruglyak V V 2012 *Appl. Phys. Lett.* **101** 152402
[10] Tkachenko V S, Kuchko A N and Kruglyak V V 2013 *Low Temperature Physics* **39** 163
[11] Gaididei Y, Kravchuk V P and Sheka D D 2014 *Phys. Rev. Lett.* **112** 257203
[12] Yoneya M, Kuboki K and Hayashi M 2008 *Phys. Rev.* B **78** 064419
[13] Pylypovskyi O V, Kravchuk V P, Sheka D D, Makarov D, Schmidt O G and Gaididei Y 2014 Magnetochiral symmetry breaking in a Möbius ring (arXiv:1409.2049)
[14] Landeros P and Núñez Á S 2010 *J. Appl. Phys.* **108** 033917
[15] Napoli G and Vergori L 2012 *Phys. Rev. Lett.* **108** 207803
[16] Napoli G and Vergori L 2012 *Phys. Rev.* E **85** 061701
[17] Dzialoshinskii I E 1957 *Sov. Phys. JETP* **5** 1259–72
[18] Dzyaloshinsky I 1958 *Journal of Physics and Chemistry of Solids* **4** 241–55
[19] Slastikov V V and Sonnenberg C 2012 *IMA J. Appl. Math.* **77** 220–35
[20] Hertel R 2013 *SPIN* **03** 1340009
[21] Kläui M, Vaz C A F, Lopez-Diaz L and Bland J A C 2003 *J. Phys.: Condens. Matter* **15** 985–1024
[22] Guimarães A P 2009 Principles of Nanomagnetism *NanoScience and Technology* (Berlin Heidelberg: Springer)
[23] Olver F W J, Lozier D W, Boisvert R F and Clark C W (ed) 2010 *NIST Handbook of Mathematical Functions* (New York: Cambridge University Press)
[24] Giesen F, Podbielski J and Grundler D 2007 *Phys. Rev.* B **76** 014431
[25] Demokritov S 2009 *Spin Wave Confinement* (Singapore: World Scientific) ISBN 981-4241-06-7
[26] Kravchuk V P, Sheka D D and Gaididei Y B 2007 *J. Magn. Magn. Mater.* **310** 116–25
[27] González A, Landeros P and Núñez Á S 2010 *J. Magn. Magn. Mater.* **322** 530–5
[28] Yan M, Andreas C, Kakay A, Garcia-Sanchez F and Hertel R 2011 *Appl. Phys. Lett.* **99** 122505